

Numerically Modelling Blockage Effects on the Flow Between Flat Plates

M.D. Griffith, K. Hourigan and M.C. Thompson

Department of Mechanical Engineering
Monash University, Clayton, VIC, 3800, AUSTRALIA

Abstract

Results are reported for a two-dimensional numerical investigation of the effect of various semi-circular blockages on the laminar flow between two plates, for Reynolds number between 50 and 3000, and blockage ratio ranging from 0.05 to 0.9. The study is undertaken with the intention of providing a fundamental understanding of blockage effects in arterial constrictions, or stenoses. The results with blockage ratio of 0.5 compare favourably with previous work on the flow over a backward-facing step. The two-dimensional parameter space for Reynolds number and blockage ratio is also mapped out. The analysis suggests that the onset of three-dimensionality of the flow is likely to be closely matched with that previously established for backward-facing step flow. Flow phenomena associated with blockage ratios above and below the customary half-blockage are summarised, including smaller-than-expected flow separation lengths for lower blockages, and vortex shedding and unusual structures within the recirculation zones for higher blockages.

Introduction

The study of blockage effects in internal flows has typically focused on determining correction factors for small blockage ratios in wind tunnels. The standard study of the flow over a backward-facing step closely matches a half-blocked flow, but such studies tend to be more interested in the various instabilities that occur in the flow, rather than on any effects the step height may have. This study examines the flow behaviour between two flat plates, with the addition of a semi-circular blockage, of variable size, attached to one side. The blockage ratio is defined as $b = r/D$, where r is the radius of the semi-circular blockage and D is the distance between the two plates. Figure 1 shows one of the computational meshes used, with a blockage ratio of 0.7. Such a study has particular relevance to the flow through arterial constrictions, but also to industrial applications involving pipe flow.



Figure 1: Computational mesh, showing macroelements, used for blockage ratio = 0.7.

The subject of this study bears much similarity to the flow over a backward-facing step, of which there is a far greater availability of literature. This is due to the fact that it offers one of the simplest and most well-defined occurrences of separated flow. The standard test-section geometry is well-known, consisting of a channel with a sudden expansion. This expansion causes an immediate separation of the flow, along with the appearance of a recirculation zone. The work of Armaly *et al.* [1] offers a detailed review of the subject, including an experimental investigation with a fixed expansion ratio of 0.516, and Reynolds numbers ranging through the laminar, turbulent and transitional regimes. With increasing Reynolds number in the laminar regime, the length of the first recirculation zone also in-

creased, and was accompanied by the appearance, downstream, of more recirculation zones on alternating sides of the channel. Three-dimensional effects were also observed.

Numerical studies of the problem, as in [2, 3, 4], give good accounts of the development of unsteadiness and three-dimensionality in the flow, and are important in determining the limitations of two-dimensional analyses. The work of Williams and Baker [10] is particularly useful, in its comparison of two and three-dimensional numerical simulations of backward-facing step flow. For the geometry used in the present two-dimensional study, the exact onset of three-dimensionality in the flow is unknown and must be kept in consideration. The work of Thangam and Knight [8] seems to present the only study of the effects of step height. They found a strong dependence of recirculation length on step height, with a Reynolds number based on the width of, and maximum velocity in, the small inlet, before the expansion.

An investigation focusing on higher blockage effects was carried out by Sahin and Owens' [6], but it used the geometry of a freely suspended cylinder between two plates, and was more interested in how the problem related to cases of unbounded flow past cylinders. Although the geometry bears only a limited similarity to this study (it is symmetrical and creates a wake consisting of twin vortices) Sahin and Owens work showed that the proximity of the walls would increase the critical Reynolds number at which shedding would occur. Also of some interest is the work of Marquillie and Ehrenstein [5], which examines the flow over a bump on a flat plate. Their work, having no blockage effects, showed that at high Reynolds number, the flow became unsteady, with smaller zones of recirculation shedding off the end of the main recirculation zone.

This paper will firstly give a brief outline of the method used in the study, followed by a description of the various flow behaviours occurring over the parameter space.

Method

Problem Definition

Figure 1 shows a section of the macro-element mesh used for the cases run with blockage ratio of 0.7. Similar meshes were produced for blockage ratios from 0.05 to 0.9. The Reynolds number is based on the hydraulic diameter ($2D$) and is described by:

$$Re = \frac{2DU_{ave}}{\nu} \quad (1)$$

where U_{ave} is the average flow velocity between the plates at inlet and ν denotes the kinematic viscosity. Data cited from other studies have been rescaled to fit this Reynolds number definition. A fully-developed Poiseuille profile, with a non-dimensionalised average velocity of 1, and a peak of 1.5, was prescribed at the inlet, such that:

$$U = 6y(1-y) \quad (2)$$

where the bottom and top walls are placed at $y=0$ and $y=1$, respectively. The inlet was placed six plate widths ($6D$) upstream

of the bump, and the outlet 25 widths downstream. Increasing distances beyond these values produced no discernible effect on the near-wake behaviour.

Tests were done over a broad range of Reynolds number, with the main restriction being the higher velocities generated over the semi-circular blockage. Blockage ratios ranging from 0.05 to 0.9 were used. For the lower blockage ratios, runs were made for Reynolds numbers ranging from 50 to 3000, whilst for higher blockages the upper limit was more restricted. The maximum Reynolds number achieved for the blockage ratio 0.9 was 500. This highlights a limitation of the two-dimensional analysis. For the flow between two flat plates, the transition to turbulence is known to begin when $Re \approx 2000$. In addition to this, the constriction of the flow over the blockage will act as an additional tripping mechanism for transition.

Numerical Method

The investigation employed a spectral-element method. Previously, the software for this method has been successfully used and validated in the prediction of wake flows past rings [7] and circular cylinders [9]. The spectral-element code uses high-order Lagrangian polynomial interpolants to approximate the solution variables for each element. Generally, a grid resolution of 49 (7×7) nodes per element was used, however for higher blockages and Reynolds numbers, elements comprising of 8×8 nodes per element had to be employed, to properly resolve parts of the flow field. Recirculation lengths and downstream vorticity profiles were the flow field characteristics used to analyse the effect of grid resolution. Increasing the nodal concentrations beyond the levels described produced no discernible effect.

Results

Flow Separation Length

Figure 2 shows the streamlines for the flow over a blockage of 0.5, at $Re = 1000$. This geometry is the closest to the classic

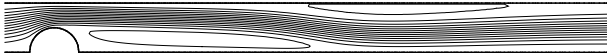


Figure 2: Streamlines for $b = 0.5$ and $Re = 1000$.

backward-facing step case and the flow behaved much as expected. For this case, two flow separation zones (FSZ's) can be seen: immediately after the blockage, and then on the top wall, beginning near where the flow reattaches on the bottom. The initial FSZ is formed by the sudden expansion at the blockage, and the subsequent adverse pressure gradient along the back half of the blockage. The length of this initial flow separation zone, L , serves as an effective way of characterising the flow behaviour. The end of the first recirculation zone, L , was determined by locating where the line of zero velocity, emanating from the flow separation point at the blockage, met the lower wall. Dividing by the blockage height, r , normalises the recirculation length for different blockage ratios.

For this blockage size and up to $Re \approx 400$, the recirculation length matched well with the data of previous studies. Above this point, the two-dimensional computational results give a recirculation length lower than previous experimental results for a backward-facing step [1]. Williams and Baker [10] have examined this problem previously in their investigation of two and three-dimensional numerical simulations for backward-facing steps. They found that the flow became three-dimensional at $Re \approx 400$, and that recirculation lengths calculated from these three-dimensional results, more closely matched the experimental results of Armaly *et al.* [1]. The onset of this three-

dimensionality can be put down to the effect of the sidewalls of the experimental apparatus. Hence, regardless of any effect caused by the different two-dimensional geometries, a divergence between the experimental and two-dimensional results at this Reynolds number is not wholly unexpected. Data is not available on when the two dimensional flow may become three-dimensional for the other blockage ratios, but the 0.5 blockage gives us some guide.

Figure 3 shows a plot of all normalised recirculation lengths for all blockages. Also depicted on the graph are the results of

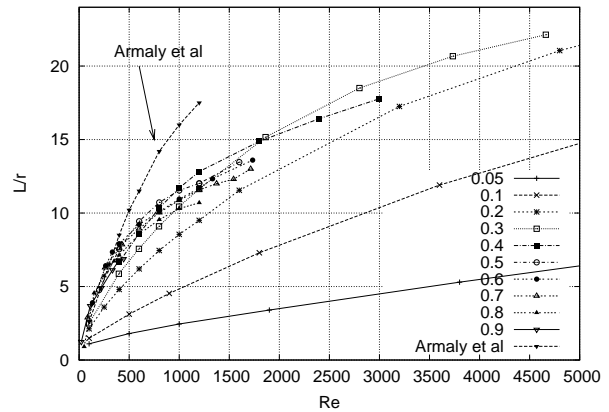


Figure 3: Plot of normalised recirculation length (L/r) against upstream Reynolds number (Re).

Armaly *et al.* [1], up to $Re = 1200$, where they observed the transitional flow regime beginning. The divergence at $Re \approx 400$ between the two data sets, at which the flow is thought to become three-dimensional, can be clearly seen, and bears a strong similarity to the comparisons made by Williams and Baker [10]. Excepting the lower blockage ratios, the data sets for each ratio appear to follow a similar curve, meaning the normalised recirculation length is largely a function of upstream Reynolds number. The work on step-height effects for a backward-facing step flow by Thangam and Knight [8] showed a much greater dependence on step height, or blockage size. However, the Reynolds number in that study was referenced to the maximum velocity before the step, which did not change with the step height. In this study, the comparable velocity, by continuity, is dependent on the blockage size. For this geometry, referencing the upstream velocity and channel width for the Reynolds number, yielded the most useful form of figure 3.

The lower blockage ratios, 0.05, 0.1 and 0.2, produced recirculation lengths lower than those for higher blockages. These results can largely be put down to the low fluid velocities at these blockage heights. If we examine equation 2, at $y = 0.05$, it returns $U_{y=0.05} = 0.285U_{ave}$. At these heights, the more rapid parts of the fluid flow over the blockage are largely unperturbed. The low fluid velocity in the vicinity of the blockage results in a smaller recirculation zone. A similar effect is either masked or not reproduced at $b = 0.9$, since the entirety of the fluid flow is forced through the tiny gap, meaning a very high velocity around the blockage. Using the local U velocity at the blockage height, calculated by equation 2, as the reference velocity for the Reynolds number, concentrates the results on figure 3 into a slightly smaller band, but doesn't allow for an easy comparison with other studies and geometries, such as backward-facing steps.

Wake behaviour

Apart from the behaviour of the initial flow separation length,

there were other flow phenomena observed in the parameter space. As observed in many backward-facing step studies, the appearance of a second FSZ on the upper wall, near the end of the initial FSZ, would occur as the Reynolds number was increased. This secondary zone results from another adverse pressure gradient, produced when the flow expands near the end of the first recirculation zone. It was found that the secondary zone of recirculation could only be produced with blockages of 0.3 and greater. For $b = 0.3$, the secondary zone appeared at $Re \approx 2200$, and for $b = 0.9$, at $Re \approx 60$. By a similar mechanism, a third zone of recirculation could be produced, but only for $b \geq 0.6$. No third recirculation zone is observed for $b = 0.5$, which is in contrast to the work of Armaly *et al.* [1], who observed the third recirculation zone for Reynolds numbers between 1200 and 2300. However, this experimental range falls within the transitional regime, which is not accounted for in the present two-dimensional investigation. Figure 4 presents a map of the parameter space, presenting the boundaries over which various phenomena occur. It includes the boundaries at which the second and third recirculation zones begin to appear. It is important to note that data is only known at 0.1 blockage intervals, boundary lines are fitted to those data and the precise critical Reynolds number for each phenomenon may not be known.

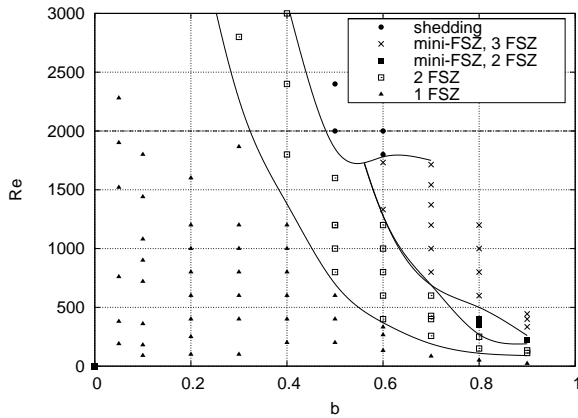


Figure 4: Map of wake behaviour over Reynolds number and blockage. Lines indicate the boundaries of each wake behaviour. Data points are also plotted.

Those data points labelled “mini-FSZ” denote the appearance at the end of the initial recirculation zone of a vortex structure, not observed in the previously cited backward-facing step investigations. This steady vortex structure is never apparent with the 0.5 blockage ratio, which is the closest geometry to the standard backward-facing step. The vortex structure makes a brief appearance with the 0.6 blockage ratio, at $Re \approx 1500$. Increasing the Reynolds number to 1800, produces vortex shedding from the blockage. The phenomenon is best observed with the 0.7 and 0.8 blockage ratios. Figure 5 shows plots of the vorticity at $b = 0.7$ and $Re = 400, 800, 1200, 1600$.

The first instance, at $Re = 400$, is located below the relevant boundary on figure 4, and the steady vortex structure is not immediately apparent. The next three instances clearly depict the appearance of the vortex structure at the end of the first recirculation zone. The structure seems to consist, initially, of a single smaller zone of recirculating flow, just behind the point at which the flow reattaches to the bottom wall. As the Reynolds number increases, a second smaller recirculating zone can be seen, particularly for $Re = 1200$. At $Re = 1600$, a third zone is apparent indicating that a series of these zones is developing upstream, as the Reynolds number is increased.

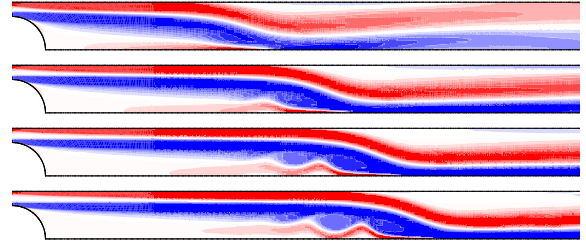


Figure 5: Visualisation of the vorticity field, at $b = 0.7$ and $Re = 400, 800, 1200, 1600$.

Figure 6, on the following page, shows a close-up of another instance of this vortex structure, this time at $b = 0.8$ and $Re = 1000$. Total velocity vectors are overlaid on the vorticity field to give a better indication of the flow behaviour. The vortex structure here seems quite complex. A series of three mini-recirculations is apparent and even the hint of a fourth is present. Closer inspection reveals the presence of further, even smaller recirculations, or mini-flow separation zones, between the obvious ones in figure 6, closer to the bottom wall. If we examine the very end of the first major recirculation zone, there exists a high reverse velocity back along the bottom wall. This flow seems to quickly separate, precipitating the appearance of the first smaller recirculation zone. Figures 5 and 6 suggest that an increase in Reynolds number promotes the continued development of the vortex pattern, right up until the onset of vortex shedding from the blockage. The steadiness of this vortex structure was initially surprising. Tests were performed and the steady state did not respond to small perturbations in the flow, higher mesh resolutions or longer outlet lengths.

The points labelled “shedding” on figure 4 represent those simulations where the flow sheds vortices from the blockage. The different vortex dynamics, on and above the corresponding boundary, have not yet been fully analysed. In comparison to Sahin and Owens work [6], the onset of shedding is delayed to a much higher Reynolds number ($Re \approx 1800$, rather than $Re \approx 340$). This is to be expected, as there is only one large vortex forming behind the asymmetric blockage of this study, as compared to the far more unstable twin vortices behind the cylinder in Sahin and Owens’ study. There is a possible comparison here, in the occurrence of delayed shedding. The proximity of the top wall to the blockage may be having a suppressing effect on shedding, much as the proximity of the two walls does on the shedding from the Sahin and Owens cylinder [6]. Looking again at figure 4, we see that, up to the 0.5 blockage, the gradient of the boundary for the appearance of shedding, at least partially, continues in the boundary for the appearance of the apparent new vortex structure in the initial flow separation zone. The appearance and growth of this structure in the initial flow separation zone as Reynolds numbers and blockage ratios increase, may indicate an increasing, yet delayed, propensity for shedding to begin.

If we consider that Armaly *et al.* observed the transition to turbulence commencing at $Re = 1200$ for a 0.5 blockage ratio on a backward-facing step [1], we could reasonably surmise that the critical Reynolds number for transition would be even lower for higher blockage ratios. The blockage’s effectiveness as a tripping mechanism would only increase with the size of the blockage. Taking this into consideration, it is possible the instability in the initial flow separation zone, as shown in figure 6, only occurs above where the transition to turbulence would occur. The instability may be an indication that the flow at these Reynolds number is no longer two-dimensional and perhaps the same vortex structure would not be reproduced in any three-dimensional

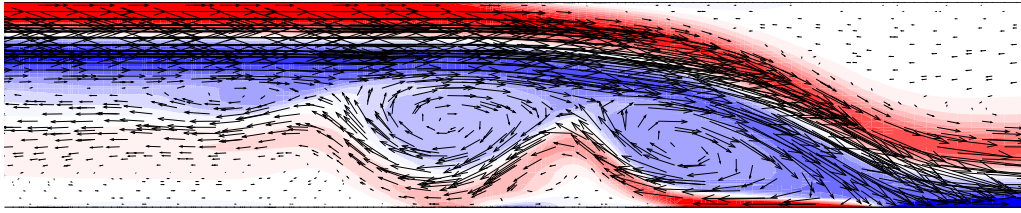


Figure 6: Close-up of the end of the initial FSZ for $b = 0.8$ and $Re = 1000$. Vorticity is plotted, with total velocity vectors overlaid.

simulations or experiments. Work on the similarities and differences between two and three-dimensional simulations for high blockage ratios, similar to that by Williams and Baker [10] on a backward-facing step of 0.5 blockage ratio, is not available and, for now, can only be estimated.

Conclusions

A numerical investigation of the two-dimensional laminar flow over semi-circular blockages has been carried out. Comparisons have been made with studies of the flow over a backward-facing step, which bears several similarities to the geometry used in this study. The results for $b = 0.5$ compared favourably with the experimental work of Armaly *et al.* [1] and the numerical simulations of Williams and Baker [10]. The lengths of the initial flow separation were closely matched with the experimental work, up to $Re \approx 400$, where the onset of three-dimensionality is thought to occur. Excepting the smaller blockage ratios, for a constant upstream Reynolds number, the normalised recirculation lengths seemed to all behave similarly. For blockage ratios equal to or less than 0.2, it was found that the low velocities around the blockages, close to the channel wall, resulted in a smaller initial recirculation zone. At higher blockage ratios, the reduction in area and the resultant high velocity through the constriction masked or cancelled out any similar effect.

For blockage ratios of 0.4 and greater, vortex shedding from the blockage was observed for higher Reynolds numbers. For blockage ratios of 0.6 and greater the appearance of a vortex structure at the end of the first recirculation zone was observed, before the onset of shedding. It was postulated that the appearance of this vortex structure was an indication of delayed or suppressed shedding. Whether the same vortex structure will be reproduced in any three-dimensional simulations or experiments is currently under investigation.

Acknowledgements

The research was principally supported by the Australian Research Council, ARC Grant No:DP0452664

References

- [1] Armaly, B.F., Durst, F., Pereira, J.C.F and Schoenung B., Experimental and Theoretical Investigation of Backward-Facing Step Flow, *J. Fluid Mech.*, **127**, 1983, 473–496.
- [2] Barkley, D., Gomes, M.G.M and Henderson, R.D., Three-Dimensional Instability in Flow over a Backward-Facing Step, *J. Fluid Mech.*, **473**, 2002, 167–190.
- [3] Kaiktis, L., Karniadakis, G.E. and Orszag, S.A., Onset of Three-Dimensionality, Equilibria, and Early Transition in Flow over a Backward-Facing Step, *J. Fluid Mech.*, **231**, 1991, 501–528.
- [4] Kaiktis, L., Karniadakis, G.E. and Orszag, S.A., Unsteadiness and Convective Instabilities in Two-Dimensional Flow over a Backward-Facing Step, *J. Fluid Mech.*, **321**, 1996, 157–187.
- [5] Marquillie, M. and Ehrenstein, U., On the onset of nonlinear oscillations in a separating boundary-layer flow, *J. Fluid Mech.*, **490**, 2003, 169–188.
- [6] Sahin, M. and Owens, R.G., A Numerical Investigation of Wall Effects up to High Blockage Ratios on Two-Dimensional Flow past a Confined Circular Cylinder, *Phys. Fluids*, **16**, 2004, 1305–1320.
- [7] Sheard, G.S., Thompson, M.C. and Hourigan, K., From Spheres to Circular Cylinders: Classification of Bluff Ring Transitions and Structure of Bluff Ring Wakes, *J. Fluid Mech.*, **492**, 2003, 147–180.
- [8] Thangam, S. and Doyle, D. D., Effect of Stepheight on the Separated Flow past a Backward Facing Step (brief communication), *Phys. Fluids A*, **1**, 1989, 604–606.
- [9] Thompson, M.C., Hourigan, K. and Sheridan, J., Three-Dimensional Instabilities in the Wake of a Circular Cylinder, *Exp. Therm. Fluid Sci.*, **12**, 1996, 190–196.
- [10] Williams, P.T. and Baker, A.J., Numerical Simulations of Laminar Flow over a 3D Backward-Facing Step, *Int. J. Numer. Methods Fluids*, **24**, 1997, 1159–1183.